

## Fission and quasifission of the composite system $Z = 114$ formed in heavy-ion reactions at energies near the Coulomb barrier

E. M. Kozulin,<sup>1</sup> G. N. Knyazheva,<sup>1</sup> T. K. Ghosh,<sup>2</sup> A. Sen,<sup>2</sup> I. M. Itkis,<sup>1</sup> M. G. Itkis,<sup>1</sup> K. V. Novikov,<sup>1</sup> I. N. Diatlov,<sup>1</sup> I. V. Pchelintsev,<sup>1</sup> C. Bhattacharya,<sup>2</sup> S. Bhattacharya,<sup>2</sup> K. Banerjee,<sup>2,\*</sup> E. O. Saveleva,<sup>1</sup> and I. V. Vorobiev<sup>1</sup>

<sup>1</sup>*Flerov Laboratory of Nuclear Reactions, Joint Institute for Nuclear Research, 141980 Dubna, Russia*

<sup>2</sup>*Variable Energy Cyclotron Centre, 1/AF Bidhan Nagar, Kolkata 700 064, India*



(Received 28 September 2018; published 22 January 2019)

**Background:** Study of competition between compound nucleus fission and quasifission in heavy-ion-induced reactions and its dependence on the reaction entrance channel are important for picking up the right target-projectile combination for the synthesis of superheavy elements.

**Purpose:** We investigate the decrease of fusion probability in the  $^{52}\text{Cr} + ^{232}\text{Th}$  reaction in comparison with that in the reactions  $^{48}\text{Ca} + ^{244}\text{Pu}$  and  $^{48}\text{Ti} + ^{238}\text{U}$ . All reactions lead to the formation of composite systems with  $Z = 114$ .

**Methods:** Mass-energy distributions of binary fragments formed in the reaction  $^{52}\text{Cr} + ^{232}\text{Th}$  leading to the  $^{284}\text{Fl}$  composite system at energies of 265, 288, 302, and 320 MeV have been measured using the double-arm time-of-flight spectrometer CORSET. To study the properties and entrance channel dependence of quasifission in more detail, the mass and energy distributions of fragments formed in the  $^{86}\text{Kr} + ^{198}\text{Pt}$  reaction, leading to the same composite system  $^{284}\text{Fl}$ , have also been measured.

**Results:** The contribution of symmetric fragments in all fissionlike events is nearly the same for both the reactions  $^{48}\text{Ti} + ^{238}\text{U}$  and  $^{52}\text{Cr} + ^{232}\text{Th}$  at energies above the barrier, while it is greater for  $^{48}\text{Ca} + ^{244}\text{Pu}$ . The analysis of total kinetic energy distribution of symmetric fragments formed in the reaction  $^{52}\text{Cr} + ^{232}\text{Th}$  shows that at an energy 15% over the Bass barrier the contribution of compound nucleus fission in the capture cross section is less than 0.4%.

**Conclusions:** The fusion probability drops down by about a factor of 4 at the transition from the  $^{48}\text{Ca} + ^{244}\text{Pu}$  reaction to  $^{48}\text{Ti} + ^{238}\text{U}$  and about a factor of 25 at the transition to  $^{52}\text{Cr} + ^{232}\text{Th}$  at energies above the barrier. It agrees with the trend of fusion probability to decrease exponentially with increasing the mean fissility parameter of the composite system.

DOI: [10.1103/PhysRevC.99.014616](https://doi.org/10.1103/PhysRevC.99.014616)

### I. INTRODUCTION

Recently great success has been achieved in the synthesis of new superheavy elements (SHEs) formed in complete fusion of heavy nuclei. At present, both cold (where one of the reaction partners is  $^{208}\text{Pb}$  or  $^{209}\text{Bi}$ ) and hot (using  $^{48}\text{Ca}$  ions) fusion reactions have been used to produce SHEs. The formation cross sections of new SHEs with  $Z = 112$ – $118$  obtained in the reactions with  $^{48}\text{Ca}$  ions are of the order of a few picobarns [1–4], while in the cold fusion reactions the cross sections drop rapidly with increasing element number, and the cross section for Nh ( $Z = 113$ ) is about 55 fb [5]. Further progress in synthesis of new SHEs using cold fusion reactions is hindered due to this dramatic decrease of the formation cross sections.

The fusion reactions of actinide targets with  $^{48}\text{Ca}$  ions have a number of advantages. The excitation energy of 30–40 MeV

of the formed compound nucleus (CN) at the interaction energies near the Coulomb barrier and the neutron excess of  $^{48}\text{Ca}$  allow one to obtain more neutron-rich nuclei than in the case of the cold fusion reactions. However, since the actinide nuclei are not stable and their half-lives decrease with increasing the element number, the heaviest actinide nucleus that may be used in the hot fusion reactions is  $^{249}\text{Cf}$ . Consequently, the heaviest SHE that may be produced in reactions of  $^{48}\text{Ca}$  ions with actinide nuclei is Og ( $Z = 118$ ).

A possible alternative pathway is represented by the complete fusion of actinide nuclei with heavier projectiles such as Ti, Cr, Fe, or Ni leading to the formation of compound nuclei with  $Z = 118$ – $126$  and  $N = 178$ – $188$ . The excitation energies of the CN formed in these reactions are about 30–40 MeV at the Coulomb barrier energy, which allows one to observe  $3n$  and  $4n$  evaporation residue (ER) channels (similar to  $^{48}\text{Ca}$ -induced reaction) and makes these reactions suitable for synthesis of new SHEs. However, at the transition to heavier projectiles, an increase of the Coulomb repulsion between the interacting nuclei gives rise to the quasifission (QF) and deep-inelastic processes, which strongly suppress the CN formation.

\*Present address: Department of Nuclear Physics, Research School of Physical Sciences and Engineering, Australian National University, Canberra ACT 2601, Australia.

QF is considered as a “bridge between deep-inelastic collisions and complete fusion reactions” [6,7]. Nevertheless, it is difficult to distinguish the QF and deep-inelastic collisions (DICs) since both the processes are binary with full momentum transfer, in which the composite system separates in two main fragments without forming a CN and are characterized by sufficient energy dissipation and mass transfer. The angular distributions of DICs are focused mainly near the angles of grazing collisions and DIC evolution time is a few zeptoseconds, while the QF is characterized by smoother angular distributions and its evolution time can extend up to tens of zeptoseconds.

To estimate fusion probability  $P_{\text{CN}}$  (the probability that after overcoming the Coulomb barrier the interacting nuclear system reaches a compact CN) both experimental and theoretical approaches can be applied. At present it is established that  $P_{\text{CN}}$  depends strongly on the reaction entrance channel, incident energy, and angular momentum and shows the general dependence on the fissility of the composite system. However, it can differ by one order of magnitude at similar values of the fissility parameter. The theoretical models, applied to describe the whole evolution of low-energy nucleus-nucleus collisions with strong channel coupling leading to deep-inelastic scattering, CN formation, and QF, describe rather well the ER cross sections for already measured reactions [8–12]. Nevertheless, the calculated values of  $P_{\text{CN}}$  differ by one order of magnitude [13,14]. Moreover, for the region of unexplored nuclear systems these predictions differ from each other by several orders of magnitude. For instance, the predicted production cross sections of SHEs with  $Z = 120$ , formed in the  $^{50}\text{Ti} + ^{249}\text{Cf}$  and  $^{54}\text{Cr} + ^{248}\text{Cm}$  reactions, differ by a factor of more than 100 [12,15–18].

Efforts to synthesize superheavy element  $Z = 120$  with a  $^{58}\text{Fe}$  beam at GSI and  $^{64}\text{Ni}$  beams at Dubna were unsuccessful. A  $^{54}\text{Cr}$  beam was considered to be an alternate option. In an attempt to produce the element at GSI [19] in the  $^{54}\text{Cr} + ^{248}\text{Cm}$  reaction, a possible assignment to the decay of an isotope of element 120 was discussed. However, recent reanalysis of the data could not confirm it [20]. Experimental determination of  $P_{\text{CN}}$  can improve the understanding of the underlying reaction mechanisms.

In this paper the mass and energy distributions of binary fragments formed in the reactions  $^{52}\text{Cr} + ^{232}\text{Th}$  and  $^{86}\text{Kr} + ^{198}\text{Pt}$  leading to the same composite system  $^{284}\text{Fl}$  ( $Z = 114$ ) at energies near the Coulomb barrier have been measured and compared with the reactions  $^{48}\text{Ca} + ^{238}\text{U}$  [21,22],  $^{48}\text{Ca} + ^{244}\text{Pu}$  [22], and  $^{48}\text{Ti} + ^{238}\text{U}$  [23] leading to the formation of similar composite systems  $^{286}\text{Cn}$ ,  $^{292}\text{Fl}$ , and  $^{286}\text{Fl}$ , to estimate the decrease of fusion probability at the transition from the reactions with  $^{48}\text{Ca}$  ions to the  $^{48}\text{Ti}$ - and  $^{52}\text{Cr}$ -induced reactions.

## II. ENTRANCE CHANNEL PROPERTIES OF THE STUDIED REACTIONS

The entrance channel properties of the reactions under study related to the competition between quasifission and fusion-fission processes, such as Coulomb factor  $Z_p Z_t$ , mean fissility parameter  $x_m$ , and mass asymmetry  $\alpha_0 = (A_t - A_p)/(A_t + A_p)$ , are listed in Table I. The mean

TABLE I. The entrance channel properties for the reactions under study:  $Z_p Z_t$  is the Coulomb factor,  $x_m$  is the mean fissility parameter, and  $\alpha_0$  is the entrance channel mass asymmetry.

Reaction	System	$Z_p Z_t$	$x_m$	$\alpha_0$
$^{86}\text{Kr} + ^{198}\text{Pt}$	$^{284}\text{Fl}$	2808	0.917	0.394
$^{52}\text{Cr} + ^{232}\text{Th}$	$^{284}\text{Fl}$	2160	0.846	0.634
$^{48}\text{Ti} + ^{238}\text{U}$	$^{286}\text{Fl}$	2024	0.823	0.664
$^{48}\text{Ca} + ^{244}\text{Pu}$	$^{292}\text{Fl}$	1880	0.780	0.671
$^{48}\text{Ca} + ^{238}\text{U}$	$^{286}\text{Cn}$	1840	0.770	0.664

fissility parameter, defined as a linear combination between the effective fissility parameter of the entrance channel and fissility parameter of the compound nucleus,  $x_m = 0.25x_{\text{CN}} + 0.75x_{\text{eff}}$ , was recently proposed in Ref. [24] as a possible criterion to identify the reaction mechanism. The effective fissility parameter of the entrance channel  $x_{\text{eff}}$ , defined as

$$x_{\text{eff}} = \frac{4Z_p Z_t / (A_p^{1/3} A_t^{1/3} (A_p^{1/3} + A_t^{1/3}))}{50.883(1 - 1.7826(\frac{A_{\text{CN}} - 2Z_{\text{CN}}}{A_{\text{CN}}})^2)},$$

is connected with repulsive and attractive forces in the entrance channel, and the fissility parameter of the compound nucleus  $x_{\text{CN}}$ , defined as

$$x_{\text{CN}} = \frac{Z_{\text{CN}}^2 / A_{\text{CN}}}{50.883(1 - 1.7826(\frac{A_{\text{CN}} - 2Z_{\text{CN}}}{A_{\text{CN}}})^2)},$$

reflects the stability of the CN with respect to fission.

From the analysis of mass-energy distributions of fissionlike fragments formed in the reactions  $^{48}\text{Ca} + ^{238}\text{U}$  and  $^{48}\text{Ca} + ^{244}\text{Pu}$  [21,22] it was shown that though QF is the dominating process for both the reactions even at interaction energies above the Coulomb barrier the CN-fission contribution in the formation of symmetric fragments with  $A_{\text{CN}}/2 \pm 20\text{u}$  is about 70 and 50%, respectively. For the reactions  $^{48}\text{Ti} + ^{238}\text{U}$  and  $^{52}\text{Cr} + ^{232}\text{Th}$  the values of the mean fissility parameter  $x_m$  and the Coulomb factor  $Z_p Z_t$  are larger than those for the reactions with  $^{48}\text{Ca}$  ions that would lead to an increase of the QF contribution in the former reactions. However, the entrance channel properties do not change as dramatically as for the case of the  $^{86}\text{Kr} + ^{198}\text{Pt}$  reaction and the decrease of the CN-formation cross section in the reactions with  $^{48}\text{Ti}$  and  $^{52}\text{Cr}$  ions is expected to be not as strong as for  $^{86}\text{Kr} + ^{198}\text{Pt}$ .

According to the systematic study of various nuclear interaction mechanisms and their dependence on the reaction entrance channel [25], the dominant process expected for the reaction  $^{86}\text{Kr} + ^{198}\text{Pt}$  is QF. The measurements of mass, energy, and angular distributions of binary fragments formed in a similar reaction  $^{84}\text{Kr} + ^{208}\text{Pb}$  [26–28] have shown that DICs and QF are the main reaction mechanisms. Moreover, the ER cross section for the neighboring nucleus  $^{278}\text{Nh}$  produced in the reaction  $^{70}\text{Zn} + ^{209}\text{Bi}$  is at the level of tens of femtobarns [5], which is three orders of magnitude lower than that in the case of the reactions with  $^{48}\text{Ca}$  ions [1–4]. Consequently, the CN formation in the reaction  $^{86}\text{Kr} + ^{198}\text{Pt}$  is expected to

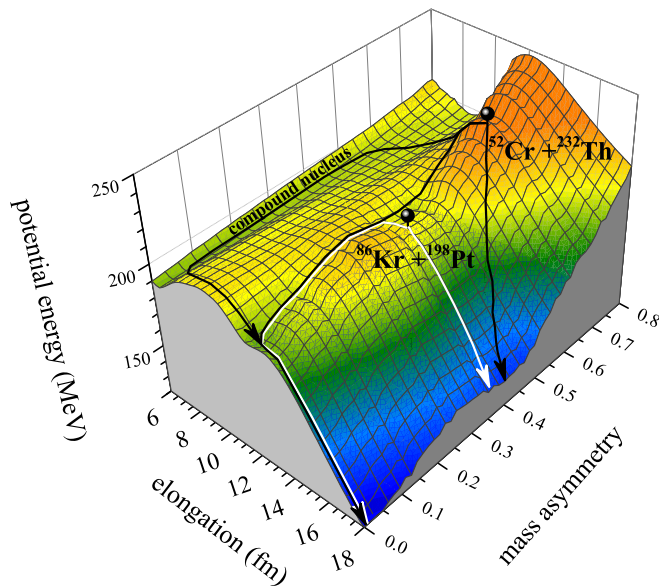


FIG. 1. Potential energy surface for the nuclear system  $^{284}\text{Fl}$  as a function of elongation and mass asymmetry. Injection configurations (contact points) for  $^{52}\text{Cr} + ^{232}\text{Th}$  and  $^{86}\text{Kr} + ^{198}\text{Pt}$  are shown by the circles. Arrows show schematically the QF and CN-formation trajectories.

be negligibly small. Nevertheless, the analysis of the mass and energy distributions of fragments formed in this reaction, which leads to the formation of the same composite system as in the case of  $^{52}\text{Cr} + ^{232}\text{Th}$ , can provide important information about the properties of the QF fragments. That allows us to disentangle the QF events from all fissionlike fragments more reliably and to estimate more precisely the fusion probability for the  $^{52}\text{Cr} + ^{232}\text{Th}$  system.

The potential energy surface for the  $^{284}\text{Fl}$  nuclear system as a function of elongation and mass asymmetry calculated in the framework of the two-center shell model using the NRV project [29] is shown in Fig. 1. Two minima in the exit channel connected with the influence of closed shells at  $Z = 82$ ,  $N = 126$  (responsible for the formation of asymmetric QF fragments) and  $Z = 50$ ,  $N = 82$  (symmetric QF) are observed. It is clearly seen from Fig. 1 that for the  $^{86}\text{Kr} + ^{198}\text{Pt}$  reaction, due to the position of the contact point on the driving potential surface, the formed composite system goes directly to the scission point via asymmetric and symmetric QF valleys, whereas in the case of the  $^{52}\text{Cr} + ^{232}\text{Th}$  reaction the system can also evolve along the valley leading to the CN formation on par with symmetric and asymmetric QF valleys.

It should be noted that actinide nuclei are strongly deformed. It is known that in the reactions with well-deformed nuclei their mutual orientation affects considerably the reaction dynamics [30–34], namely, near-tip collisions of deformed nuclei lead to QF, while the near-side collisions yield a gain in fusion probabilities even at large values of  $Z_p Z_t$  [23]. Recently it was found that the orientation effect caused by strong deformation of the colliding nuclei also plays an important role in the formation of the QF reaction fragments [35]. Since  $^{238}\text{U}$  and  $^{232}\text{Th}$  are well-deformed nuclei, we may expect an increase of fusion probability at energies above the

barrier for near-side collisions in the reactions  $^{48}\text{Ti} + ^{238}\text{U}$  and  $^{52}\text{Cr} + ^{232}\text{Th}$  as in the case of the reactions with  $^{48}\text{Ca}$  ions.

### III. EXPERIMENT

The experiments were performed at the Flerov Laboratory of Nuclear Reactions at the U400 and U400M cyclotrons. Beams of 265, 288, 302, and 320 MeV of  $^{52}\text{Cr}$  ions struck a layer of  $^{232}\text{Th}$  280  $\mu\text{g}/\text{cm}^2$  deposited on 35- $\mu\text{g}/\text{cm}^2$  carbon backing. A beam of 465 MeV of  $^{86}\text{Kr}$  ions struck a layer of  $^{198}\text{Pt}$  200  $\mu\text{g}/\text{cm}^2$  deposited on 1.3- $\mu\text{m}$  titanium backing. During the experiments the target backings faced the beam. The energy resolution was  $\sim 1\%$ . Beam intensities on the target were 1–2 pA. The enrichment of the targets was 99.99%. The details of measurements for the reactions with  $^{48}\text{Ca}$  and  $^{48}\text{Ti}$  ions are given in [22,23].

For all studied reactions the binary reaction products were detected in coincidence by the double-arm time-of-flight spectrometer CORSET [36]. Each arm of the spectrometer consists of a compact start detector and a position-sensitive stop detector, both based on microchannel plates. The acceptance of the spectrometer in the reaction plane was  $\pm 12^\circ$ . The spectrometer arms were positioned in an optimal way according to the kinematics of the reaction and their angles were adjusted several times to account for change in beam energy during the experiment. The position resolution of the stop detectors equals  $0.3^\circ$ , and the time resolution is about 150 ps. The mass and energy resolutions of the CORSET setup have been deduced from the full width at half maximum of the mass and energy spectra of the elastic particles, respectively. In the above conditions, the mass resolution of the spectrometer is  $\pm 2$  u; the total kinetic energy (TKE) resolution is  $\pm 10$  MeV.

The data processing assumes standard two-body kinematics [36]. Primary masses, velocities, energies, and angles of reaction products in the center-of-mass system were calculated from the measured velocities and angles using the momentum and mass conservation laws with the assumption that the mass of the composite system is equal to  $M_{\text{target}} + M_{\text{projectile}}$ . Neutron evaporation before scission was not taken into account. This is justified by the fact that even at the highest reaction energies not more than four neutrons could be emitted. Hence, considering that the spectrometer resolution is  $\pm 2$  u, the neutron emission will not lead to visible effects on the mass-energy distributions. Corrections for the fragment energy losses through the target material, target backing, and start detector foils were included in the data analysis.

Extraction of the binary reaction channels with full momentum transfer and removal of products of sequential and incomplete fission reactions, induced fission of the target, and targetlike nuclei, or reactions on impurity atoms in the target, were based on the analysis of the kinematics diagram (see [36,37] for details).

### IV. RESULTS AND DISCUSSION

Mass-total kinetic energy (M-TKE) distributions of the primary binary fragments obtained in the reactions  $^{52}\text{Cr} + ^{232}\text{Th}$  and  $^{86}\text{Kr} + ^{198}\text{Pt}$  at energies above the Bass barrier are shown in Fig. 2. The distributions for the reactions  $^{48}\text{Ca} + ^{244}\text{Pu}$  [22] and  $^{48}\text{Ti} + ^{238}\text{U}$  [23] are also presented. All these reactions

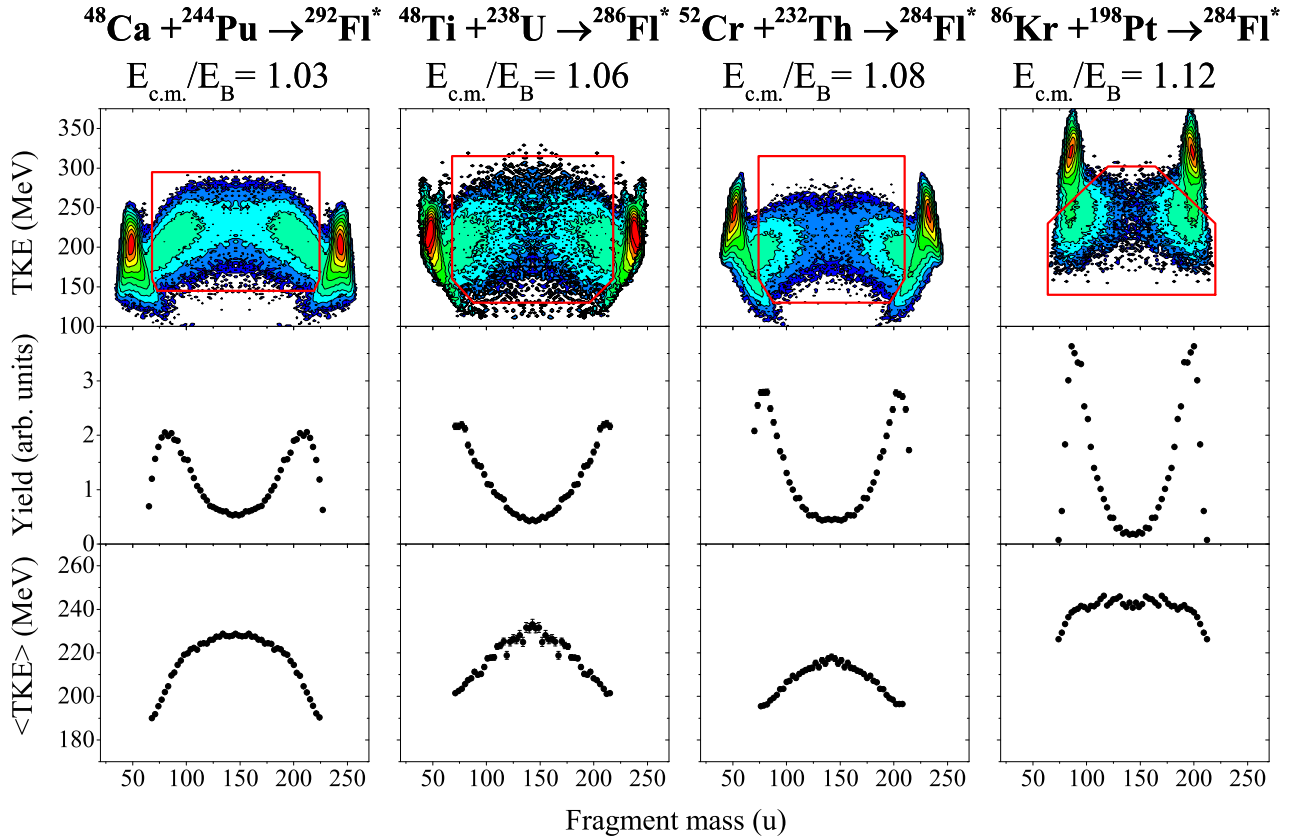


FIG. 2. The mass and energy distributions of binary fragments formed in the reactions  $^{48}\text{Ca} + ^{244}\text{Pu}$ ,  $^{48}\text{Ti} + ^{238}\text{U}$ ,  $^{52}\text{Cr} + ^{232}\text{Th}$ , and  $^{86}\text{Kr} + ^{198}\text{Pt}$  leading to the formation of composite systems with  $Z = 114$  at energies above the Bass barrier. From top to bottom: The M-TKE matrices of binary reaction products, the mass distributions, and the average total kinetic energy as a function of mass of fissionlike fragments inside the contour line on M-TKE matrices.

lead to the formation of composite systems with  $Z = 114$ . In the M-TKE distributions the reaction products with masses close to those of the projectile and target are associated with elastic and quasielastic events and were not considered in the present analysis. The measurements for the reactions  $^{48}\text{Ca} + ^{244}\text{Pu}$ ,  $^{48}\text{Ti} + ^{238}\text{U}$ , and  $^{52}\text{Cr} + ^{232}\text{Th}$  have been done at correlation angles lower than the angle for grazing collisions, therefore the contribution of DIC events is insignificant. Reaction products located between the quasielastic peaks are assumed as totally relaxed events, i.e., as fissionlike fragments, and can originate either from CN-fission or QF processes. The events selected are those within the contour lines in the M-TKE distributions in Fig. 2.

Mass-energy distributions of fragments formed in the reaction  $^{86}\text{Kr} + ^{198}\text{Pt}$  at energy  $E_{\text{lab}} = 465$  MeV have been integrated over the laboratory angles from  $30^\circ$  up to  $68^\circ$ . The angle of grazing collisions for this system at this energy is  $74.3^\circ$ . One can see from Fig. 2 that the main part of fissionlike fragments lies near the masses of target and projectile nuclei. The angular distributions for these fragments peak around the grazing angles typical for DICs, whereas for more symmetric fragments they show no dependence on the scattering angle that can indicate the presence of a slower process.

At first glance the mass-energy distributions are similar for the reactions with  $^{48}\text{Ca}$ ,  $^{48}\text{Ti}$ , and  $^{52}\text{Cr}$  ions. The clearly

pronounced asymmetric QF component with heavy fragments near the double magic lead is observed. The drift of asymmetric QF to the mass symmetry, estimated as a difference between the projectile mass and more symmetric mass at the half-maximum yield of QF, decreases from 61 u for the reaction with  $^{48}\text{Ca}$ , to 50 u for  $^{48}\text{Ti}$ , to 46 u for  $^{52}\text{Cr}$ , to 15 u for  $^{86}\text{Kr}$ . From the analysis of experimental mass and angular distributions of fissionlike fragments formed in the reactions with  $^{238}\text{U}$  ions it was found [6] that the mass drift to the symmetry shows the characteristics of an overdamped motion with a universal time constant independent of the scattering system and bombarding energy. We have deduced the mean reaction times for the asymmetric QF process for the studied systems using the relation between the mean reaction time and mass drift proposed in Ref. [6]. The mean reaction times for  $^{48}\text{Ca} + ^{244}\text{Pu}$ ,  $^{48}\text{Ti} + ^{238}\text{U}$ ,  $^{52}\text{Cr} + ^{232}\text{Th}$ , and  $^{86}\text{Kr} + ^{198}\text{Pt}$  are about 6.2, 5.0, 4.8, and 2.7 zs, respectively. Thus, the heavier the ion the smaller the QF reaction time.

The average TKE ( $\langle\text{TKE}\rangle$ ) dependence on fragment mass differs even more. In the reactions with  $^{48}\text{Ca}$  and  $^{48}\text{Ti}$  the values of the average TKE are very close to each other; however, in the case of the  $^{48}\text{Ti}$ -induced reaction the  $\langle\text{TKE}\rangle$  decreases much faster with the mass asymmetry than for the  $^{48}\text{Ca}$ -induced reaction. In the case of  $^{52}\text{Cr}$  ions the  $\langle\text{TKE}\rangle$  for symmetric fragments is considerably lower compared to

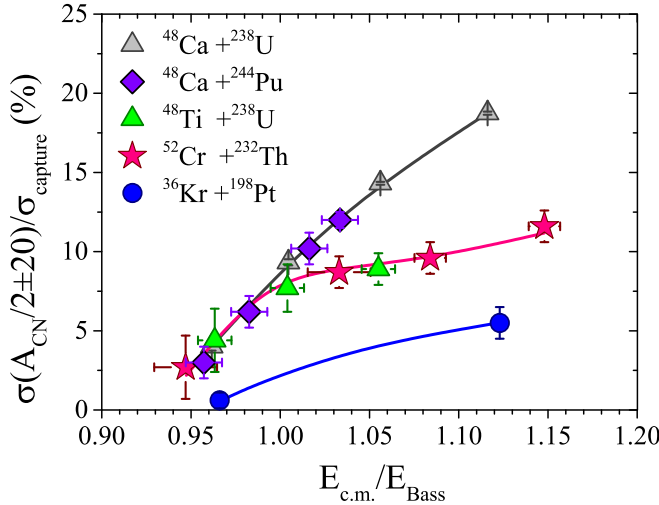


FIG. 3. The contribution of symmetric fragments in all fission-like events formed in the reactions  $^{48}\text{Ca} + ^{238}\text{U}$ ,  $^{48}\text{Ca} + ^{244}\text{Pu}$ ,  $^{48}\text{Ti} + ^{238}\text{U}$ ,  $^{52}\text{Cr} + ^{232}\text{Th}$ , and  $^{86}\text{Kr} + ^{198}\text{Pt}$  in dependence on the interaction energy.

$^{48}\text{Ca}$ - and  $^{48}\text{Ti}$ -induced reactions, which points to the prevailing asymmetric QF process even in this mass region. For the  $^{86}\text{Kr} + ^{198}\text{Pt}$  reaction, the  $\langle\text{TKE}\rangle$  virtually does not depend on the mass of the formed fragments and is substantially higher than one can expect for the  $^{284}\text{Fl}$  compound nucleus. The total kinetic energy loss ( $\text{TKEL} = E_{\text{c.m.}} - \text{TKE}$ ), observed in this reaction, is about 90 MeV. Nevertheless, despite this rather large TKEL, a full kinetic energy dissipation does not occur. This means that in the case of the  $^{86}\text{Kr} + ^{198}\text{Pt}$  reaction we deal with a faster process not compatible with the compound nucleus formation.

At the transition from  $^{48}\text{Ca}$  to  $^{48}\text{Ti}$  and  $^{52}\text{Cr}$  ions the contribution of symmetric fragments decreases also. However, even in the case of  $^{86}\text{Kr} + ^{198}\text{Pt}$  (where the QF is a major process and CN formation is negligible) the symmetric fragments are observed. The measurements of the mass-angle distributions showed that to form such fragments the composite system should exist for more than  $10^{-20}$  s [6,7]. This time is long enough for compound nucleus formation. As a first step to evaluate the CN-fission cross section the contribution of fragments with masses  $A_{\text{CN}}/2 \pm 20$  u can be considered. According to the liquid drop model (LDM) the mass distributions of the CN-fission fragments for the systems with  $Z \sim 108$ –114 can have the symmetric Gaussian shape with the standard deviation of about 20 u [see, for example, [37] for the case of the Hs ( $Z = 108$ ) nucleus]. Due to the influence of the closed shells with  $Z = 50$  and  $N = 82$  the asymmetric shape of mass distribution is also possible as in the case of fission of actinides [38]. Nevertheless, in both cases the width of CN-fission fragment mass distributions does not exceed 40 u and the choice of the mass range of  $A_{\text{CN}}/2 \pm 20$  u is reasonable.

Figure 3 shows the relative contributions of symmetric fragments in capture cross sections for the reactions  $^{48}\text{Ca} + ^{244}\text{Pu}$ ,  $^{48}\text{Ti} + ^{238}\text{U}$ ,  $^{52}\text{Cr} + ^{232}\text{Th}$ , and  $^{86}\text{Kr} + ^{198}\text{Pt}$  and their dependence on the interaction energy. The same data

for the  $^{48}\text{Ca} + ^{238}\text{U}$  reaction, leading to the formation of a composite system with  $Z = 112$ , are also presented since this reaction has been extensively studied at a wide energy range below and above the Bass barrier [6,22,39]. For the reaction  $^{48}\text{Ca} + ^{244}\text{Pu}$  the experimental data are available only up to the energy of  $1.04E_{\text{Bass}}$ . It is clearly seen from Fig. 3 that the yields of symmetric fragments are similar for the reactions with  $^{48}\text{Ca}$ ,  $^{48}\text{Ti}$ , and  $^{52}\text{Cr}$  at energies below the Bass barrier. However, at energies above the barrier in the case of the reactions with  $^{48}\text{Ca}$  ions, the contribution of symmetric fragments increases monotonically, while for the reactions with  $^{48}\text{Ti}$  and  $^{52}\text{Cr}$  ions it virtually does not change and is about 8–9%. This may indicate a significant increase of the QF process at the transition from  $^{48}\text{Ca}$  to  $^{48}\text{Ti}$  and  $^{52}\text{Cr}$  ions. For the  $^{52}\text{Cr} + ^{232}\text{Th}$  reaction at energies higher than  $1.1E_{\text{Bass}}$  a small growth of the symmetric fragment contribution is observed. Unfortunately, for the reaction  $^{48}\text{Ti} + ^{238}\text{U}$  the measurements have been done only up to an energy of  $1.05E_{\text{Bass}}$ , which makes it impossible to establish this dependence at higher energies.

The contribution of symmetric fragments in all the damped reaction products (inside the contour lines in the M-TKE matrix in Fig. 2) in the reaction  $^{86}\text{Kr} + ^{198}\text{Pt}$  increases from 0.5% at the energy below the barrier to 5.5% at an energy of  $1.12E_{\text{Bass}}$ . Although for the  $^{86}\text{Kr} + ^{198}\text{Pt}$  reaction this contribution is considerably lower compared to the  $^{48}\text{Ti} + ^{238}\text{U}$  and  $^{52}\text{Cr} + ^{232}\text{Th}$  reactions, it is relatively large at the above-barrier energy. For example, in the reaction  $^{64}\text{Ni} + ^{238}\text{U}$  [21] this contribution is only 5%, despite this reaction being more asymmetric and the Coulomb factor being smaller ( $Z_1Z_2 = 2576$ ) compared to  $^{86}\text{Kr} + ^{198}\text{Pt}$ . To form symmetric fragments in the reaction  $^{86}\text{Kr} + ^{198}\text{Pt}$  about 50 nucleons have to be transferred from the target to the projectile nucleus, needing a smaller reaction time than in the  $^{48}\text{Ti} + ^{238}\text{U}$ ,  $^{52}\text{Cr} + ^{232}\text{Th}$ , and  $^{64}\text{Ni} + ^{238}\text{U}$  reactions, where the transfer of about 90–95 nucleons is needed.

The absolute differential cross sections for all fissionlike events observed in the reactions  $^{48}\text{Ca} + ^{238}\text{U}$ ,  $^{244}\text{Pu}$ ,  $^{48}\text{Ti} + ^{238}\text{U}$ , and  $^{52}\text{Cr} + ^{232}\text{Th}$  were measured at a center-of-mass angle  $\theta_{\text{c.m.}}$  of about  $90^\circ$ . Capture cross sections for all fissionlike events were estimated assuming that the angular distribution is proportional to  $1/\sin\theta_{\text{c.m.}}$ . This procedure seemed the most reasonable since the measured angular distributions are not available at present, nor is any model (theory) for the angular distribution of fragments produced in the QF process. The capture cross sections for the reactions  $^{48}\text{Ca} + ^{238}\text{U}$ ,  $^{244}\text{Pu}$ , and  $^{48}\text{Ti} + ^{238}\text{U}$  have been already reported in [21–23]. The cross sections for the reaction  $^{52}\text{Cr} + ^{232}\text{Th}$  at energies around the Coulomb barrier have been measured in this paper. The absolute capture cross sections together with the cross sections of symmetric ( $A_{\text{CN}}/2 \pm 20$  u) fragment formation for the reactions  $^{48}\text{Ca} + ^{238}\text{U}$  [21],  $^{48}\text{Ca} + ^{244}\text{Pu}$  [22],  $^{48}\text{Ti} + ^{238}\text{U}$  [23], and  $^{52}\text{Cr} + ^{232}\text{Th}$  are presented in Fig. 4. It is clearly seen that the capture cross sections decrease at the transition from the  $^{48}\text{Ca}$ -induced reactions to the reactions with the  $^{48}\text{Ti}$  and  $^{52}\text{Cr}$  ions. At energies above the barrier the capture cross section for  $^{48}\text{Ca} + ^{238}\text{U}$  is close to the geometrical one; for the  $^{48}\text{Ti} + ^{238}\text{U}$  and  $^{52}\text{Cr} + ^{232}\text{Th}$  reactions it is about 60% of the geometrical cross section.

At energies above the barrier the symmetric fragment formation cross section decreases by a factor of 2 for

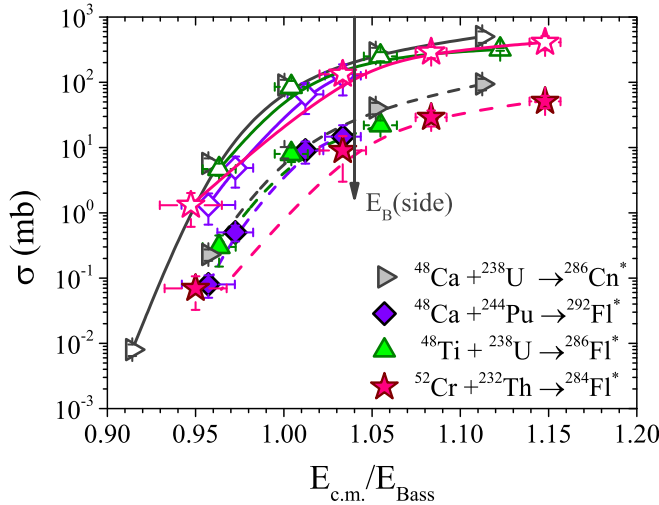


FIG. 4. The capture cross sections (open symbols) and the cross sections of symmetric fragments with masses  $A_{CN}/2 \pm 20u$  (filled symbols) for the reactions  $^{48}\text{Ca} + ^{238}\text{U}$  [21],  $^{48}\text{Ca} + ^{244}\text{Pu}$  [22],  $^{48}\text{Ti} + ^{238}\text{U}$  [23], and  $^{52}\text{Cr} + ^{232}\text{Th}$  in dependence on the interaction energy.

$^{48}\text{Ti} + ^{238}\text{U}$  and a factor of 4 for  $^{52}\text{Cr} + ^{232}\text{Th}$  compared to the reaction  $^{48}\text{Ca} + ^{238}\text{U}$ . Moreover, as was mentioned above, a significant part of the symmetric fragments may originate in the QF process. Therefore, only the upper limit for the CN-fission cross section can be obtained. Energy distribution gives important information about energy dissipation during the evolution of the composite system and can be used as an additional observable (together with fragment mass) to estimate the contribution of the CN-fission component into the capture cross section when the presence of other processes together with CN fission in the symmetric mass region is expected. We assume that the mass-symmetric fragments may be formed by three different modes: CN fission, symmetric QF, and a tail of asymmetric QF process.

It is well known that for CN fission of hot nuclei the TKE of fragments depends on the fissility of the CN and does not depend on the interaction energy [40]. The most probable value of TKE may be estimated using the Viola systematics [41]. The deviation of average TKE from the Viola systematics for the symmetric fragments formed in the reactions  $^{48}\text{Ca} + ^{238}\text{U}$ ,  $^{48}\text{Ti} + ^{238}\text{U}$ ,  $^{52}\text{Cr} + ^{232}\text{Th}$ , and  $^{86}\text{Kr} + ^{198}\text{Pt}$  and its dependence on the interaction energy are presented in Fig. 5. In the case of the reaction  $^{48}\text{Ca} + ^{238}\text{U}$  at energies above the Coulomb barrier the average TKEs are close to the Viola systematics. It was shown in Ref. [22] that about 70% of all symmetric fragments formed in this reaction may be assigned to the CN-fission process, although the asymmetric and symmetric QF fragments are also observed. For the  $^{48}\text{Ti} + ^{238}\text{U}$  and  $^{52}\text{Cr} + ^{232}\text{Th}$  reactions the values of average TKE increase with increasing interaction energy but they are lower than the Viola predictions for these CNs even at energies well above the Coulomb barrier. As was shown in Ref. [22] for the reaction  $^{48}\text{Ca} + ^{238}\text{U}$  the average TKE of asymmetric QF virtually does not change with the collision energy. However, in the present paper it is found that for the reaction  $^{52}\text{Cr} +$

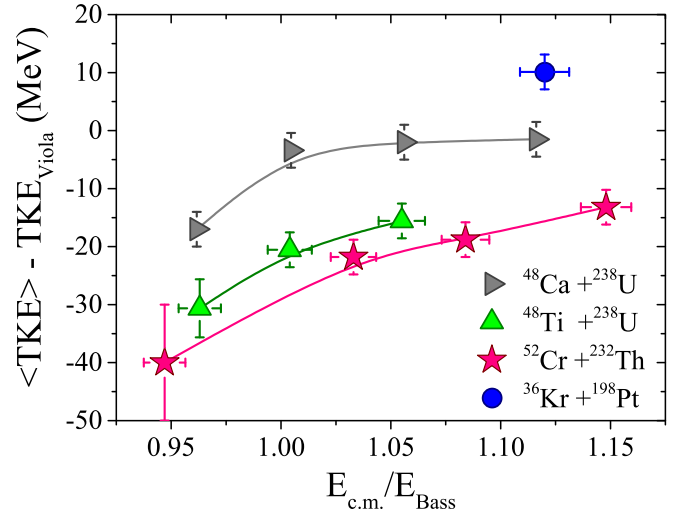


FIG. 5. The deviation of average TKE from the Viola systematics for the symmetric fragments formed in the reactions  $^{48}\text{Ca} + ^{238}\text{U}$  [21],  $^{48}\text{Ti} + ^{238}\text{U}$  [23],  $^{52}\text{Cr} + ^{232}\text{Th}$ , and  $^{86}\text{Kr} + ^{198}\text{Pt}$  in dependence on the interaction energy.

$^{232}\text{Th}$  the average TKE of asymmetric QF increases linearly with increasing interaction energy from 190 MeV at an energy of  $0.95 E_{Bass}$  to 204 MeV at  $1.15 E_{Bass}$ . Nevertheless the TKE for asymmetric QF is lower than expected for CN fission for the reactions  $^{48}\text{Ca} + ^{244}\text{Pu}$ ,  $^{48}\text{Ti} + ^{238}\text{U}$ , and  $^{52}\text{Cr} + ^{232}\text{Th}$  even at energies above the barrier (see Fig. 2). Similar to multimodal fission where the influence of closed shells leads to a higher TKE than that of the LDM component, for the symmetric QF, caused by the strong influence of closed shells at  $Z = 50$  and  $N = 82$ , one may expect a higher value of average TKE compared to CN fission. The lower values of average TKE compared to the Viola systematics may indicate that in the reactions  $^{48}\text{Ti} + ^{238}\text{U}$  and  $^{52}\text{Cr} + ^{232}\text{Th}$  the major part of fragments in the symmetric mass region originates from the asymmetric QF process.

One can see from Fig. 6 that the standard deviation of TKE distribution of fragments with masses  $200 \pm 10u$  formed in the asymmetric QF process virtually does not change with increasing interaction energy. The variance of TKE distribution of asymmetric QF fragments decreases with increasing mass of the projectile. For instance, for the same composite system  $^{284}\text{Fl}$  the standard deviation is about 20 MeV for the reaction with  $^{52}\text{Cr}$  ions and only 18.5 MeV for  $^{86}\text{Kr}$  ions. In the case of the  $^{286}\text{Fl}$  composite system formed in the reaction  $^{48}\text{Ti} + ^{238}\text{U}$  it is about 23 MeV. This behavior of TKE variance may be connected with the position of the contact point on the driving potential surface of the composite system. The longer the path between the contact and scission points, the greater the variance of the energy distribution is expected. It is clearly seen from Fig. 1 that for the  $^{86}\text{Kr} + ^{198}\text{Pt}$  reaction the path from the contact to the scission point via the asymmetric QF valley is much shorter than for the  $^{52}\text{Cr} + ^{232}\text{Th}$  reaction.

The standard deviations of TKE of the symmetric fragments with masses  $A_{CN}/2 \pm 20u$  are also shown in Fig. 6. The behavior of TKE variance is more complicated than in the case of asymmetric fragments. For the reaction  $^{52}\text{Cr} + ^{232}\text{Th}$

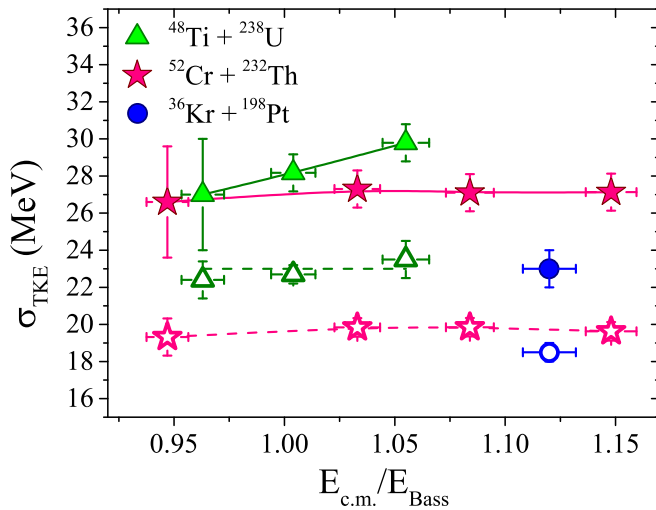


FIG. 6. The standard deviation of TKE distributions of symmetric fragments with masses  $A_{CN}/2 \pm 20$  u (filled symbols) and asymmetric fragments with masses  $200 \pm 10$  u (open symbols) formed in the reactions  $^{48}\text{Ti} + ^{238}\text{U}$  [23],  $^{52}\text{Cr} + ^{232}\text{Th}$ , and  $^{86}\text{Kr} + ^{198}\text{Pt}$  in dependence on the interaction energy.

the TKE variance virtually does not depend on interaction energy, while in the case of the reaction  $^{48}\text{Ti} + ^{238}\text{U}$  it increases slightly with increasing interaction energy. The relative contributions of different processes (CN fission and asymmetric and symmetric QF) into the formation cross section of symmetric fragments change with increasing interaction energy that influences the properties of the TKE distributions. In the case of  $^{86}\text{Kr} + ^{198}\text{Pt}$  the TKE variance is much lower than for  $^{52}\text{Cr} + ^{232}\text{Th}$ , while the average TKE is higher. Such behavior of the TKE distribution for the  $^{86}\text{Kr} + ^{198}\text{Pt}$  reaction may be connected with the dominance of symmetric QF in the formation of the symmetric fragments. This is also correlated with a shorter interaction time for the  $^{86}\text{Kr} + ^{198}\text{Pt}$  system.

As was mentioned above, the contribution of symmetric fragments to all fissionlike events virtually does not change for the reactions  $^{48}\text{Ti} + ^{238}\text{U}$  and  $^{52}\text{Cr} + ^{232}\text{Th}$  at energies above the Coulomb barrier, while for the reactions with  $^{48}\text{Ca}$  ions an increasing trend, connected with increasing contribution of the CN-fission component, is observed. Along with the features of TKE distributions found for the reactions  $^{48}\text{Ti} + ^{238}\text{U}$  and  $^{52}\text{Cr} + ^{232}\text{Th}$  this indicates that for these systems the ratio between CN fission and QF does not change virtually with increasing interaction energy. However, the lower values of average TKE and its variance in the case of the  $^{52}\text{Cr} + ^{232}\text{Th}$  reaction compared to  $^{48}\text{Ti} + ^{238}\text{U}$  indicate the increase of the asymmetric QF contribution for the former reaction, although the asymmetric QF is the main process for the both systems.

TKE distributions of the symmetric fragments with masses  $A_{CN}/2 \pm 20$  u for the reactions  $^{52}\text{Cr} + ^{232}\text{Th}$  and  $^{86}\text{Kr} + ^{198}\text{Pt}$  at energies above the barrier are presented in Fig. 7. For the reaction  $^{52}\text{Cr} + ^{232}\text{Th}$  the TKE distribution shows a two-humped shape as in the case of the  $^{48}\text{Ti} + ^{238}\text{U}$  and  $^{64}\text{Ni} + ^{238}\text{U}$  reactions [23]. Notice that in the reactions of actinide nuclei with  $^{48}\text{Ca}$  ions the TKE distributions have nearly

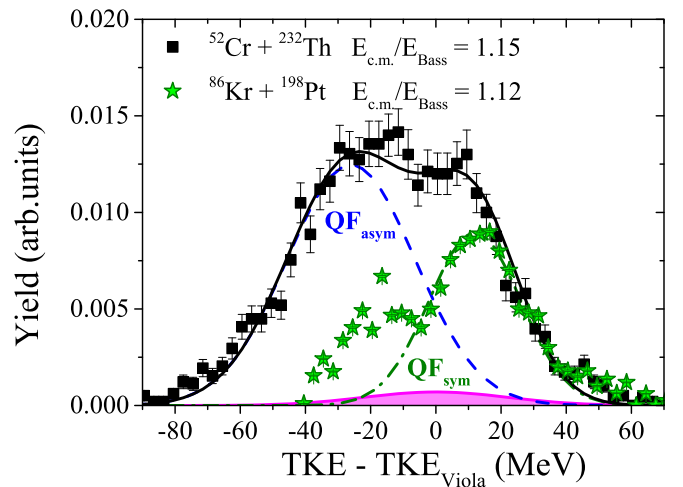


FIG. 7. TKE distributions of fragments with masses  $A_{CN}/2 \pm 20$  u for the reactions  $^{52}\text{Cr} + ^{232}\text{Th}$  (squares) and  $^{86}\text{Kr} + ^{198}\text{Pt}$  (stars) leading to the formation of the same composite system  $^{284}\text{Fl}$  at energies above the Coulomb barrier. The filled region corresponds to the TKE distribution for CN fission for  $^{52}\text{Cr} + ^{232}\text{Th}$ . The dashed and dash-dotted curves are associated with asymmetric and symmetric QF, respectively.

Gaussian shape with mean values close to those expected for the CN-fission process [22]. In the case of  $^{86}\text{Kr} + ^{198}\text{Pt}$  also, the TKE distribution is a two-humped shape with a pronounced high-energy component.

To evaluate the contribution of the CN-fission process in the symmetric mass region, the TKE distribution for the reaction  $^{52}\text{Cr} + ^{232}\text{Th}$  at an energy of  $1.15E_{\text{Bass}}$  was decomposed as a sum of three Gaussians. One of them is associated with the CN-fission process. We fix the mean value and variance of this component to the values predicted from the systematics for CN fission presented in Refs. [41] and [40], respectively. The low-energy component is attributed to asymmetric QF, while the high-energy one is connected with symmetric QF. As was shown in Ref. [37] in the case of the  $^{58}\text{Fe} + ^{208}\text{Pb}$  reaction (where the asymmetric QF is the main process even in the symmetric mass region) the variance of TKE for QF does not depend on the mass of the QF fragments. Thus, in the fitting procedure we fix the variance of the asymmetric QF component equal to the experimental value of TKE variance for the fragment mass corresponding to the maximum yield of asymmetric QF. The parameters for the symmetric QF component were deduced from the decomposition of the TKE distribution for the  $^{86}\text{Kr} + ^{198}\text{Pt}$  reaction.

The uncertainties in the deduced  $P_{\text{CN}}$  values are defined by the statistical errors of the measured TKE distribution and the parameter standard errors of the fitting procedure. In our case the Gaussians describing the yields of the different processes overlap, which unfortunately leads to a large uncertainty in deducing the area of the peak associated with CN fission. Nevertheless, fixing the mean value and variance of the symmetric QF component to the values obtained for the  $^{86}\text{Kr} + ^{198}\text{Pt}$  reaction, where the symmetric QF peak is well pronounced and hence the fitting procedure is straightforward, helps to reduce this uncertainty. In the case of the

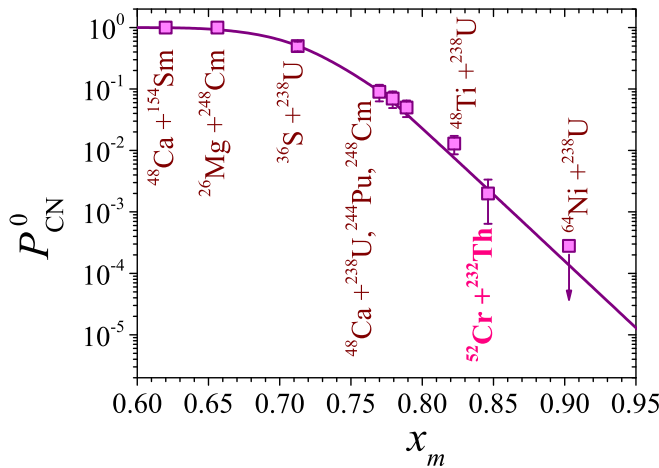


FIG. 8. Fusion probability for the reaction  $^{52}\text{Cr} + ^{232}\text{Th}$  in comparison with fusion probabilities in hot fusion reactions [23] at energies above the Coulomb barrier in dependence on the mean fissility parameter.

$^{52}\text{Cr} + ^{232}\text{Th}$  reaction the systematic error (parameter standard error derived in the fitting procedure for the area of the peak) is 70% for the CN-fission component.

According to this decomposition of TKE distribution in symmetric QF, asymmetric QF, and CN-fission components, for the reaction  $^{52}\text{Cr} + ^{232}\text{Th}$  the contribution of the CN fission is about 4% in the mass region  $A_{\text{CN}}/2 \pm 20$  u. The upper limit for CN fission for the  $^{52}\text{Cr} + ^{232}\text{Th}$  reaction at this energy is only 0.4% of the capture cross section. The CN-fission cross section estimated for the  $^{48}\text{Ca} + ^{238}\text{U}$  reaction is about 15% of the capture cross section. Hence, the CN-fission cross section drops by about a factor of 40 at the transition from  $^{48}\text{Ca} + ^{238}\text{U}$  to  $^{52}\text{Cr} + ^{232}\text{Th}$ .

The dependence of fusion probability on the mean fissility parameter for the hot fusion reactions with strongly deformed targets, deduced from the analysis of mass-energy distributions in Ref. [23], is shown in Fig. 8. The solid line in Fig. 8 is the description of fusion probability for hot fusion reactions according to an equation proposed by Zagrebaev (see [23] for details). The obtained fusion probability for the reaction  $^{52}\text{Cr} + ^{232}\text{Th}$  at energy above the Coulomb barrier ( $1.15E_{\text{Bass}}$ ) is also presented in Fig. 8. For all these reactions the target nuclei are well deformed. The  $P_{\text{CN}}$  for all presented systems has been obtained as the ratio between the yields of CN fission and the contact cross sections, which is close to the geometrical one at above-barrier collision energies. Normalization to the contact cross section instead of the capture cross section allows us to avoid the inaccuracies connected with disentangling the fissionlike fragments from elastic and quasielastic events in mass-energy distributions of binary reaction fragments, as well as with the angular integration of mass distributions for these fragments.

## V. SUMMARY

The complete fusion probability for the formation of SHEs has been investigated in the reactions of  $^{52}\text{Cr}$  ions with actinide nuclei at energies around the Coulomb barrier and compared with the same for the reactions with  $^{48}\text{Ca}$  and  $^{48}\text{Ti}$  ions. The mass and energy distributions of binary fragments formed in the  $^{52}\text{Cr} + ^{232}\text{Th}$  and  $^{86}\text{Kr} + ^{198}\text{Pt}$  reactions, leading to the formation of the same composite system  $^{284}\text{Fl}$ , have been studied for this purpose. The measurements were performed using the double-arm time-of-flight spectrometer CORSET.

Due to the entrance channel properties for the  $^{86}\text{Kr} + ^{198}\text{Pt}$  reaction quasifission is the major process, while the contribution of the CN-fission component is negligibly small. The measurements of mass and energy distributions of fragments formed in this reaction help us to analyze the properties of quasifission fragments formed in the other reactions leading to the same  $^{284}\text{Fl}$  composite system, in which, due to the entrance channel properties, the other reaction mechanisms together with QF are also present.

It was found that for the  $^{52}\text{Cr} + ^{232}\text{Th}$  reaction the asymmetric quasifission is a dominant process at all measured energies below and above the Coulomb barrier. The contribution of symmetric fragments to all fissionlike events is similar to the  $^{48}\text{Ti} + ^{238}\text{U}$  reaction leading to the formation of the  $^{286}\text{Fl}$  composite system. At energies above the barrier, it virtually does not change with increasing interaction energy and is about 8–9% for reactions with  $^{48}\text{Ti}$  and  $^{52}\text{Cr}$  ions. In contrast, for the reactions of actinide nuclei with  $^{48}\text{Ca}$  ions the contribution of symmetric fragments increases monotonically. This may indicate a significant increase of the QF process at the transition from  $^{48}\text{Ca}$  to  $^{48}\text{Ti}$  and  $^{52}\text{Cr}$  ions.

The fusion probability for the reaction  $^{52}\text{Cr} + ^{232}\text{Th}$  at an energy 15% over the Bass barrier has been estimated from the analysis of mass and TKE distributions. The obtained fusion probability is in good agreement with the phenomenological fusion probability dependence on the mean fissility parameter found for the reactions of well-deformed nuclei with  $^{36}\text{S}$ ,  $^{48}\text{Ca}$ ,  $^{48}\text{Ti}$ , and  $^{64}\text{Ni}$  ions. It is found that at energies above the Coulomb barrier the fusion probability drops by about a factor of 4 at the transition from the  $^{48}\text{Ca} + ^{244}\text{Pu}$  reaction to  $^{48}\text{Ti} + ^{238}\text{U}$  and about a factor of 25 at the transition to  $^{52}\text{Cr} + ^{232}\text{Th}$ .

## ACKNOWLEDGMENTS

We thank the staff of the U400 cyclotron for their careful work. This work was supported by the Russian Foundation for Basic Research (Grant No. 15-52-45098) and Department of Science and Technology, Government of India (Grant No. INT/RUS/RFBR/P185). S.B. acknowledges with thanks the financial support received as Raja Ramanna Fellow from the Department of Atomic Energy, Government of India.

[1] Y. T. Oganessian *et al.*, *Phys. Rev. C* **70**, 064609 (2004).  
[2] Y. T. Oganessian *et al.*, *Phys. Rev. C* **74**, 044602 (2006).

[3] Y. T. Oganessian, *J. Phys. G* **34**, R165 (2007).  
[4] Y. T. Oganessian *et al.*, *Phys. Rev. Lett.* **104**, 142502 (2010).



- [5] K. Morita *et al.*, *J. Phys. Soc. Jpn.* **73**, 2593 (2004).
- [6] W. Q. Shen *et al.*, *Phys. Rev. C* **36**, 115 (1987).
- [7] J. Toke *et al.*, *Nucl. Phys. A* **440**, 327 (1985).
- [8] V. Zagrebaev and W. Greiner, *J. Phys. G* **31**, 825 (2005).
- [9] Y. Aritomo, K. Hagino, K. Nishio, and S. Chiba, *Phys. Rev. C* **85**, 044614 (2012).
- [10] C. Simenel, *Eur. Phys. J. A* **48**, 152 (2012).
- [11] G. G. Adamian, N. V. Antonenko, and W. Scheid, *Nucl. Phys. A* **678**, 24 (2000).
- [12] A. K. Nasirov, G. Mandaglio, G. Giardina, A. Sobiczewski, and A. I. Muminov, *Phys. Rev. C* **84**, 044612 (2011).
- [13] W. Loveland, *J. Phys. Conf. Ser.* **420**, 012004 (2013).
- [14] R. Yanez, W. Loveland, J. S. Barrett, L. Yao, B. B. Back, S. Zhu, and T. L. Khoo, *Phys. Rev. C* **88**, 014606 (2013).
- [15] Z. H. Liu and Jing-Dong Bao, *Phys. Rev. C* **80**, 054608 (2009).
- [16] V. Zagrebaev and W. Greiner, *Phys. Rev. C* **78**, 034610 (2008).
- [17] G. G. Adamian, N. V. Antonenko, and W. Scheid, *Eur. Phys. J. A* **41**, 235 (2009).
- [18] K. Siwek-Wilczynska, T. Cap, and J. Wilczynski, *Int. J. Mod. Phys. E* **19**, 500 (2010).
- [19] S. Hofmann *et al.*, *Eur. Phys. J. A* **52**, 180 (2016).
- [20] F. P. Heßberger and D. Ackermann, *Eur. Phys. J. A* **53**, 123 (2017).
- [21] E. M. Kozulin *et al.*, *Phys. Lett. B* **686**, 227 (2010).
- [22] E. M. Kozulin, G. N. Knyazheva, S. N. Dmitriev, I. M. Itkis, M. G. Itkis, T. A. Loktev, K. V. Novikov, A. N. Baranov, W. H. Trzaska, E. Vardaci, S. Heinz, O. Beliuskina, and S. V. Khlebnikov, *Phys. Rev. C* **89**, 014614 (2014).
- [23] E. M. Kozulin, G. N. Knyazheva, K. V. Novikov, I. M. Itkis, M. G. Itkis, S. N. Dmitriev, Y. T. Oganessian, A. A. Bogachev, N. I. Kozulina, I. Harca, W. H. Trzaska, and T. K. Ghosh, *Phys. Rev. C* **94**, 054613 (2016).
- [24] R. du Rietz, E. Williams, D. J. Hinde, M. Dasgupta, M. Evers, C. J. Lin, D. H. Luong, C. Simenel, and A. Wakhle, *Phys. Rev. C* **88**, 054618 (2013).
- [25] M. G. Itkis, E. Vardaci, I. M. Itkis, G. N. Knyazheva, and E. M. Kozulin, *Nucl. Phys. A* **944**, 204 (2015).
- [26] F. Hanappe, M. Lefort, C. Ngo, J. Peter, and B. Tamain, *Phys. Rev. Lett.* **32**, 738 (1974).
- [27] K. L. Wolf, J. P. Unik, J. R. Huizenga, J. Birkelund, H. Freiesleben, and V. E. Viola, *Phys. Rev. Lett.* **33**, 1105 (1974).
- [28] R. Vandenbosch and M. P. Webb, *Phys. Rev. C* **14**, 143 (1976).
- [29] <http://nrv.jinr.ru/nrv>
- [30] D. J. Hinde, M. Dasgupta, J. R. Leigh, J. C. Mein, C. R. Morton, J. O. Newton, and H. Timmers, *Phys. Rev. C* **53**, 1290 (1996).
- [31] G. N. Knyazheva *et al.*, *Phys. Rev. C* **75**, 064602 (2007).
- [32] V. Zagrebaev and W. Greiner, *Int. J. Mod. Phys. E* **17**, 2199 (2008).
- [33] K. Nishio, H. Ikezoe, S. Mitsuoka, I. Nishinaka, Y. Nagame, Y. Watanabe, T. Ohtsuki, K. Hirose, and S. Hofmann, *Phys. Rev. C* **77**, 064607 (2008).
- [34] A. Wakhle, C. Simenel, D. J. Hinde, M. Dasgupta, M. Evers, D. H. Luong, R. du Rietz, and E. Williams, *Phys. Rev. Lett.* **113**, 182502 (2014).
- [35] E. M. Kozulin, V. I. Zagrebaev, G. N. Knyazheva, I. M. Itkis, K. V. Novikov, M. G. Itkis, S. N. Dmitriev, I. M. Harca, A. E. Bondarchenko, A. V. Karpov, V. V. Saiko, and E. Vardaci, *Phys. Rev. C* **96**, 064621 (2017).
- [36] E. M. Kozulin *et al.*, *Instrum. Exp. Tech.* **51**, 44 (2008).
- [37] I. M. Itkis *et al.*, *Phys. Rev. C* **83**, 064613 (2011).
- [38] F. Gonnemann, *The Nuclear Fission Process* (CRC, Boca Raton, FL, 1991), Chap. 8, p. 287.
- [39] K. Nishio, S. Mitsuoka, I. Nishinaka, H. Makii, Y. Wakabayashi, H. Ikezoe, K. Hirose, T. Ohtsuki, Y. Aritomo, and S. Hofmann, *Phys. Rev. C* **86**, 034608 (2012).
- [40] M. G. Itkis and A. Ya. Rusanov, *Phys. Part. Nucl.* **29**, 160 (1998).
- [41] V. E. Viola, K. Kwiatkowski, and M. Walker, *Phys. Rev. C* **31**, 1550 (1985).